Thermocline thermal energy storage optimisation combining exergy and life cycle assessment

D. Le Roux, Yasmine Lalau, B. Rebouillat, Pierre Neveu, Régis Olivès

Thermocline thermal energy storage optimisation combining exergy and life cycle assessment

D. Le Roux [a,c], Y. Lalau [b], B. Rebouillat [a], P. Neveu [c], R. Olivès [a,c,*]

[a] Procédés, Matériaux et Energie Solaire (PROMES-CNRS), UPR 8521. Rambla de la Thermodynamique, 66 100 Perpignan, France
[b] Centre RAPSODEE, CNRS, UMR 5302, IMT Mines Albi, 81 013 Albi Cedex 9, France
[c] Université de Perpignan Via Domitia, 52 av. P. Alduy, 66100 Perpignan, France

Keywords:
Waste heat valorisation
Thermocline
Packed-bed
Thermal energy storage
Life cycle assessment
Exergy
Multi-criteria optimisation

A B S T R A C T

Thermocline thermal energy storage is one of the most promising solutions for recovering waste heat in industrial plants. This paper aims to optimise the shape of a thermal energy storage to minimise its environmental impacts and maximise its exergy efficiency. The reference storage is an existing industrial high-temperature air/ceramic packed-bed heat storage called EcoStock®. The physical model used to determine the performances of the tank is a one dimensional model with two equations: one for the heat transfer fluid and one for the filler material. The environmental impacts are analysed using a life cycle assessment through four selected indicators: cumulative energy demand, global warming potential, abiotic depletion potential and particulate matter. To solve this multi-criteria problem, a particle swarm optimisation algorithm was applied with several exergy and environmental weighting factors. A Pareto set is obtained, bounded by the single exergy or environmental optimisations. Favouring exergy efficiency reduces the volume of the tank. However, environmental footprint of the tank is increased: the indicators of cumulative energy demand and abiotic depletion potential are considerably higher. The shape of the tank evolves with the exergy weight, from a square shape (environmental optimisation) to a tapered shape (exergy optimisation).

1. Introduction

Successfully overcoming the energy and environmental transition challenges relies on three successive steps: reducing needs, increasing process efficiency and massively deploying renewable energies. Thermal Energy Storage (TES) systems should address the last two steps.

On one hand, Concentrated Solar Power (CSP) plants grew strongly in 2019, with an 11% increase in the global fleet, reaching a capacity of 6.2 GW out of the 2 588 GW of renewable energy installed worldwide. Electricity generated by CSP has been estimated at 16 TWh of the 27 011 TWh of total global electricity production in 2019 [1]. A major advantage of CSP is that it produces heat which can be more easily stored than electricity. Therefore, a TES can be integrated into CSP plants to temporarily store excess thermal energy and release it later for delayed electricity generation. This system improves the competitiveness and availability of the electricity produced and promotes the deployment of renewable energies.

On the other hand, industrial energy demand is mostly supplied by fossil fuels and consumed as heat (70% worldwide) [2]. However, up to 50% of this energy is wasted in processes: above 100 °C, 52.9 TWh/ year are lost in France [3] and 370 TWh/year in Europe [4], which represents almost 17% of total industrial consumption [5,6]. Most of the high temperature waste heat is lost in hot fumes [3], especially in steel, cement and fuel cell industries [7]. This waste heat needs to be recovered to increase the efficiency of industrial processes and provide low-impact and low-cost heat [6]. A TES system would promote the recovery of this heat by matching energy supply and demand [8].

Those two technology fields (CSP and industrial waste heat recovery) should integrate similar TES systems, operating on the same temperature range (200–600 °C) [9]. A TES system can temporarily store excess energy (for CSP) or waste heat (for industry) for later use [10]. Among the different TES systems available, two-tank technology with molten salt is the most widely used. However, the use of two tanks is costly and space consuming. These drawbacks may be improved by combining the two tanks into a single one, named a thermocline tank [11,12]. In addition to reducing the storage envelop, Thermal Energy Storage Materials (TESM) partially replace Heat Transfer Fluid (HTF) in the thermocline system. This change reduces the cost of the thermal storage media by up to 70% and the cost of the storage envelop by almost 65%

* Corresponding author at: Procédés, Matériaux et Energie Solaire (PROMES-CNRS), UPR 8521. Rambla de la Thermodynamique, 66100 Perpignan, France.
E-mail address: olives@univ-perp.fr (R. Olivès).

Nomenclature

A	Area (m^2)
c	Heat capacity $(J{\cdot}kg^{-1}{\cdot}K^{-1})$
D	Diameter (m)
Ex	Exergy (J)
ex	Specific exergy $(J{\cdot}kg^{-1})$
F_e	External shape factor $(-)$
F_i	Internal shape factor $(-)$
L	Length (m)
LCA	LCA criterion $(-)$
$\dot{m}$	Mass flow $(kg{\cdot}s^{-1})$
P	Pressure (Pa)
Q	Energy capacity (J)
S	Entropy $(J{\cdot}kg^{-1})$
t	Time (s)
T	Temperature (K)
U	Internal energy (J)
V	Volume (m^3)
z	Axial coordinates (in the direction flow) (m)

Greek symbols

Δ	Variation $(-)$
ε	Porosity $(-)$
η	Efficiency $(-)$
λ	Thermal conductivity $(W{\cdot}m^{-1}{\cdot}K^{-1})$
μ	Dynamic viscosity $(Pa{\cdot}s)$
ρ	Density $(kg{\cdot}m^{-3})$
τ	Rate $(-)$
τ_u	Utilisation rate $(-)$
ω	Weight $(-)$

Subscripts and superscripts

*	Real
∞	Outdoor or free condition
c	Charge
cutoff	Cut-off
ds	Discharge
ES	Eco-Stock®
ex	Exergy
f	Fluid
final	Final
H	High
in	In
initial	Initial
L	Low
LCA	LCA
out	Out
s	solid
t	Tank
th	Theoretical

Abbreviations

ADP	Abiotic Depletion Potential of mineral, fossil and renewable resources $(kg\ Sb_{eq})$
CED	Cumulative Energy Demand (MJ_{eq})
CSP	Concentrating Solar Power
GWP	Global Warming Potential $(kgCO_{2_{eq}})$
HTF	Heat Transfer Fluid
ILCD	International Reference Life Cycle Data system
LCA	Life Cycle Assessment
PM	Particulate Matter $(kg\ PM2.5_{eq})$
PSO	Particle Swarm Optimisation
TES	Thermal Energy Storage
TESM	Thermal Energy Storage Material
REV	Representative Elementary Volume

[13,14]. As a result, the cost of the TES can be reduced down to 35% compared to two-tank storage [15].

Many energy optimisations have been proposed on TES for CSP since the first experiments in the 1980s. First experiments on a thermocline tank showed that stratification is improved by increasing tank length to diameter ratio [16]. The first industrial thermocline storage was tested in Solar One CSP plant. This experiment proved that this technology was efficient and reliable [17]. Hoffmann *et al.* [18] studied the impact of HTF mass flow rate and filler particle diameter on energy efficiency. Ammar *et al.* [19] maximised the ratio between the stored and the pumping energies by considering three optimisation variables: tank length, particle diameter and HTF mass flow rate. Only a few studies have proposed a second law analysis to optimise thermocline systems, following Bejan [20] who states that an optimal thermal system is "the least irreversible system that the designer can afford". Krane [21] sought the optimal design and operating conditions of a TES that minimise entropy production during an entire charge–discharge cycle. Using a lumped model, Biyikoğlu [22] showed that second law efficiency can be improved by connecting TES systems in series with each other. Flueckiger *et al.* [23] studied entropy production due to conductive heat transfer, viscous dissipation and heat losses through CFD model. Rebouillat *et al.* [24] performed similar analysis, but taking into account a supplementary entropy source: the convective heat transfer between the HTF and the packing bed. They showed that the optimal geometry results in a trade-off between convective heat transfer and pressure drop. Another relevant result was the high value of the exergy efficiency of the optimised tank reaching 95%. Haller *et al.* [25] presented different indicators to assess thermal stratification in thermocline storage, based on second law analysis. Better stratification in thermocline tank increases the exergy content as well as the exergy storage capacity [26].

The lack of detailed environmental study of thermocline TES has been highlighted by Miro *et al.* [8]. In order to propose alternative energy efficient solutions, it is important to quantify and check environmental benefits by a Life Cycle Assessment (LCA). This is a standardised method (ISO 14040) that assesses the quantifiable effect of products or services on the environment throughout their life cycle [27]. LCA was firstly developed on TES in the late 2010s. The first environmental analysis on a thermocline tank proved that greenhouse gas emissions are halved compared to a two-tank storage in CSP plant [12]. A comparison of three different TES for CSP showed that sensible storage based on solid media (concrete) presents the smallest environmental footprint compared to latent storage and sensible storage using liquid media (molten salt) [28]. The use of waste materials, such as recycled ceramics [29], considerably reduced the environmental impact of TES. Natural rock can also be used as solid filler in thermocline storage, which reduced the environmental footprint compared to molten salt [30]. Although exergy and environmental optimisations exist for thermocline storage, as mentioned above, no study combines both optimisations. This is the objective of this work, which aims to evaluate and optimise the exergy and environmental performances of a thermocline TES using air as HTF and ceramics as filler material. The studied system is supposed to store waste heat from an industrial firing furnace and to release it for later use. A Particle Swarm Optimisation (PSO) algorithm [31] will be used to solve the multi-criteria optimisation problem coupling exergy efficiency maximisation and environmental impact minimisation.

2. Methodology and Data

This study seeks to optimally design a thermocline tank according to two criteria: maximising exergy efficiency and minimising environmental impacts. The exergy efficiency is evaluated using a dynamic numerical model and the environmental impacts are assessed by a LCA study. This thermocline storage is defined in the first part. Then, these two models are briefly described in this section.

2.1. Studied system

This study deals with thermocline tank system used for sensible heat storage. Fig. 1 illustrates the working principle of a thermocline tank where HTF flows through a filler material (e.g. rocks, ceramics, metals, etc.), called TESM. This HTF can be a gas, usually air, or a liquid, usually oil or molten salt. Gas is preferred for high working temperatures (above ~ 500 °C) while liquid is used for lower temperatures.

During the charging process, hot fluid is injected from the top of the tank and cold fluid is extracted from the bottom. As a result, three different zones appear: two zones have quasi-uniform temperatures (one hot at the top and one cold at the bottom), and one zone, called the thermocline, has a large temperature gradient. During the discharging process, the direction of the fluid flow is reversed. Cold fluid is injected from the bottom and hot fluid is extracted from the top. The same thermocline zone appears between the two quasi-uniform zones. In both processes, the thermocline zone moves into the tank until it is partially or completely extracted.

The objective of the present work is to optimise the environmental impacts and the exergy efficiency of an industrial tank, named Eco-Stock® [32] (Fig. 2), developed and commercialised by Eco-Tech Ceram [33], to valorise industrial waste heat. This thermocline tank uses air as HTF and ceramic balls as filler materials.

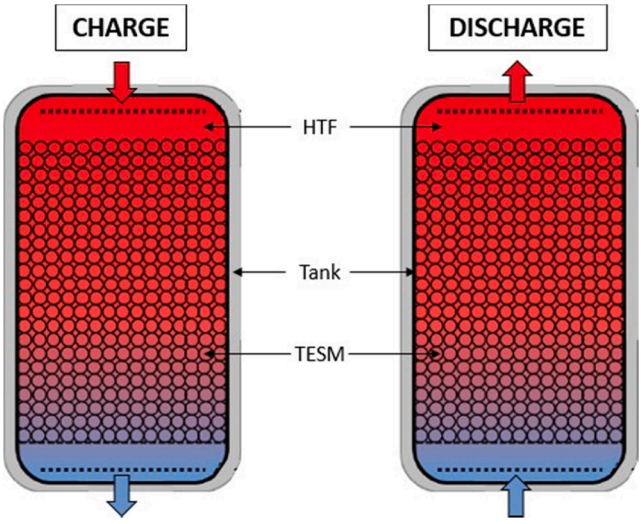

Fig. 1. Thermocline tank working principle

Fig. 2. Industrial installation of the Eco-Stock® thermal storage system

2.2. Physical model

The dynamic model is detailed in [24]. It has been developed to perform a second law analysis of thermocline TES used in CSP plant or waste heat recovery. It consists of solving transient balances of energy and entropy applied to a slice of the tank, taken as a Representative Elementary Volume (REV), as illustrated in Fig. 3. It is a one-dimensional (radial gradients are neglected) and two-phase model (HTF and filler material) that has been validated for the studied industrial tank from experimental data provided by the manufacturer [24]. The following assumptions are made:

- Fourier's law describes conductive heat transfer in the axial direction,
- Newton's law models convective heat transfer between HTF and TESM. The convective heat transfer coefficient is estimated from correlation developed for packed-bed by Wakao [34],
- Ergun's law depicts the mass transfer in the axial direction,
- The thermophysical properties of fluid and solid are constant,
- The side walls are adiabatic.

For a given HTF/TESM pair, this model evaluates the exergy behaviour and performances of the thermocline system according to five design parameters and two dimensionless optimisation variables (Table 1). The design parameters are usually given from the storage specifications: upstream and downstream processes, storage capacity, power or charge/discharge times, etc. The two optimisation variables are dimensionless shape factors, related to the geometry of the tank (ratio of diameter to length) and the particle size of the filler (ratio of particle to tank diameters).

The theoretical volume of the tank is determined from the five design parameters:

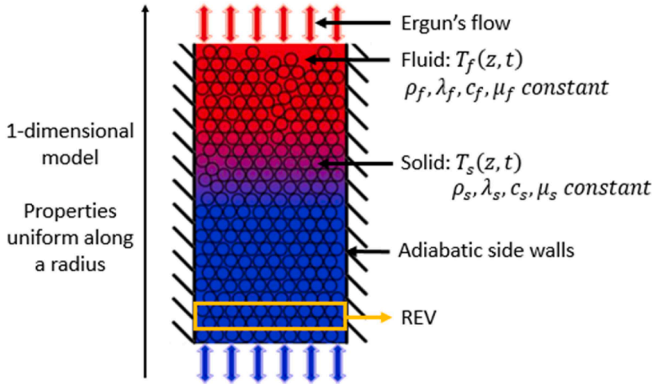

Fig. 3. Thermocline tank model [24]

Table 1
Independent variables to depict a thermocline TES

Design parameters	Optimisation variables
Theoretical storage capacity Q_{th} (J)	External shape factor $F_e = D_t / L_t$
Porosity of the packing-bed ε (-)	
Charge or discharge time t_c or t_{ds} (h) (target values)	Internal shape factor $F_i = D_s / D_t$
Operating temperatures: high T_H and low T_L (K)	

$$V_t = A_t \cdot L_t = \frac{Q_{th}}{\left(\varepsilon \cdot (\rho c)_f + (1-\varepsilon)\cdot(\rho c)_s\right)\cdot(T_H - T_L)} \quad (1)$$

With A_t: section of the tank (m^2),
L_t: length of the tank (m),
T: temperature (K),
ρ: density ($kg \cdot m^{-3}$),
c: heat capacity ($J \cdot kg^{-1} \cdot K^{-1}$).

The subscripts f and s refer respectively to the liquid and solid (filler) phases.

To model the overall performance of a thermocline tank, several cycles must be simulated to get a periodic stationary behaviour. The tank is initially discharged ($T = T_L$ uniform at $t = 0\ s$). The charging and discharging processes end when the output fluid temperature reaches the cut-off temperature respectively $T_{c,cutoff}$ and $T_{ds,cutoff}$. These temperatures are arbitrarily set at a cut-off ratio of 20% defined as follow [18,24]:

$$\Delta T_{c,cutoff} = T_H - T_{c,cutoff} = 0.2\cdot(T_H - T_L) \quad (2)$$

$$\Delta T_{ds,cutoff} = T_{ds,cutoff} - T_L = 0.2\cdot(T_H - T_L) \quad (3)$$

The thermal energy charged/discharged Q can be obtained by estimating the internal energy of the tank from the two temperatures limit profiles (i.e. begin and end of a given cycle).

$$Q = \Delta U = U_{final} - U_{initial} \quad (4)$$

For incompressible liquid and solid, internal energy of the TES write:

$$U = \int_0^{L_t} \left[\varepsilon\cdot(\rho c)_f \cdot A_t \cdot (T_f - T_L) + (1-\varepsilon)\cdot(\rho c)_s \cdot A_t \cdot (T_s - T_L)\right]\cdot dz \quad (5)$$

2.3. Performance indicator

The exergy efficiency will be used in the optimisation study defined below. It is evaluated when the stationary regime is reached. It compares the thermal power extracted from the TES by the HTF during the discharging process with that supplied to the TES by the HTF during the charging process:

$$\eta_{ex} = \frac{-\int_0^{t_{ds}} \dot{m}\cdot\Delta ex\cdot dt}{\int_0^{t_c} \dot{m}\cdot\Delta ex\cdot dt} \quad (6)$$

where t_{ds} and t_c are respectively the duration of the discharging and charging processes, $\dot{m}$ the HTF mass flow rate and Δex the specific exergy change experienced by the HTF while crossing the storage tank. For an incompressible fluid, it writes:

$$\Delta ex = c_f \cdot \left[T_{out} - T_{in} - T_\infty \cdot \ln\left(\frac{T_{out}}{T_{in}}\right)\right] + \frac{1}{\rho_f}\cdot(P_{out} - P_{in}) \quad (7)$$

where T_{in} and T_{out} are the inlet and outlet temperatures of the HTF, T_∞ the ambient temperature and P_{in} and P_{out} the inlet and outlet pressures.

2.4. Environmental impacts

Environmental impacts are calculated by a LCA, a standardised method (ISO 14040) evaluating the quantifiable effects of products or services on the environment throughout their life cycle (from "cradle-to-grave" or "cradle-to-cradle" in circular economy) [27]. The International Reference Life Cycle Data System (ILCD) 2016 mid-point method is used to calculate the LCA indicators using EcoInvent v3.5 database [35] and OpenLCA v1.8 software [36].

2.4.1. Functional unit

This study aims to quantify the environmental benefits of the optimised thermocline storage system. First, the environmental impacts of a reference case, is assessed. Then the influence of varying the optimisation variables is investigated. In this study, the reference tank is the industrial thermocline tank named Eco-Stock® (ES) [33]. The LCA of this thermocline tank with bauxite as filler material and air as HTF is based on the previous work of Lalau *et al.* [37]. A fair comparison requires a same functional unit to refer for all calculated impacts. Based on the exergy performances, the functional unit is defined as follows:

Provide a discharged thermal exergy equal to that of the reference tank ($\boldsymbol{Ex^*_{ds}} = (\boldsymbol{Ex_{ds}})_{ES} = 707\ \boldsymbol{kWh/cycle}$), during its span life (25 years) considering 1 cycle a day and 15 days off a year for maintenance.

According to this definition, the volume of the simulated tank must be determined to provide the same service defined by the functional unit. This volume is corrected from the exergy performance indicators to produce the required discharge exergy, as explained below.

The exergy utilisation ratio is used to deduce the required system size to ensure a given discharge exergy. It compares exergy charged/discharged during a cycle and the maximum exergy that can be extracted from the tank.

$$\tau_{u,ex} = \frac{\Delta Ex}{\Delta Ex_{th}} = \frac{\Delta U - T_\infty \cdot \Delta S}{\Delta U_{th} - T_\infty \cdot \Delta S_{th}} \quad (8)$$

ΔS is the real entropy change of the system, which can be deduced, as ΔU, from the pressure and temperature profiles obtained at the beginning and the end of the cycle:

$$\Delta S = S_{final} - S_{initial} \quad (9)$$

For incompressible liquid and solid, entropy of the tank writes:

$$S = \int_0^{L_t} \left[\varepsilon\cdot(\rho c)_f \cdot A_t \cdot \ln\left(\frac{T_f}{T_L}\right) + (1-\varepsilon)\cdot(\rho c)_s \cdot A_t \cdot \ln\left(\frac{T_s}{T_L}\right)\right]\cdot dz \quad (10)$$

For the theoretical value ΔS_{th}, the same expressions apply using $T_f = T_s = T_L$ for $S_{initial}$, leading to $S_{initial} = 0$, and $T_f = T_s = T_H$ for S_{final}.

The discharge exergy efficiency may be defined as the ratio between the discharge exergy quantity and the exergy charged/discharged during the cycle:

$$\eta^{ds}_{ex} = \frac{-\int_0^{t_{ds}} \dot{m}\cdot\Delta ex\cdot dt}{\Delta Ex} \quad (11)$$

The real exergy being discharged from the tank is then:

$$Ex_{ds} = -\int_0^{t_{ds}} \dot{m}\cdot\Delta ex\cdot dt = \eta^{ds}_{ex}\cdot\Delta Ex = \eta^{ds}_{ex}\cdot\tau_{u,ex}\cdot\Delta Ex_{th} \quad (12)$$

Where ΔEx_{th} writes, using Eqs. (4), (5), (9) and (10):

$$\Delta Ex_{th} = \underbrace{(A_t\cdot L_t)}_{V_t}\cdot\left[\varepsilon\cdot(\rho c)_f + (1-\varepsilon)\cdot(\rho c)_s\right]\cdot\left[(T_H - T_L) - T_\infty \cdot ln\left(\frac{T_H}{T_L}\right)\right] \quad (13)$$

In order to produce the given discharge exergy of the reference system $Ex^*_{ds} = (Ex_{ds})_{ES}$, the volume of the real tank $(V_t)^*$ must be corrected with the exergy utilisation ratios and the discharge exergy efficiencies related to the reference tank and the optimised tank:

$$(V_t)^* = (V_t)_{ES}\cdot\frac{(\eta^{ds}_{ex}\cdot\tau_{u,ex})_{ES}}{(\eta^{ds}_{ex}\cdot\tau_{u,ex})^*} \quad (14)$$

where the volume of the Eco-Stock® tank $(V_t)_{ES}$ is determined with Eq. (1).

Fig. 4. Cradle-to-grave perimeter

2.4.2. System boundaries

The scope considered in this study is "cradle-to-grave" analysis (Fig. 4). It includes all the steps from raw material extraction to the end-of-life management of the thermocline storage, through manufacturing, transport, construction, use and dismantling. All inputs and outputs of materials and energies to and from the TES system throughout its life cycle are taken into account.

The production step (raw materials + elaboration) includes the materials transport to production site. The system perimeter ends with the landfill or transport of recycled waste to the recycling plant gate. The French energy mix is considered in this study.

The inventory of the different phases of the life cycle is proportional to the optimisation variables. If the tank dimensions and/or the fluid or filler material change, so do the amount of raw materials and pressure losses.

Four LCA indicators have been selected from previous LCA concerning CSP plants and storage systems [12,37]:

- Cumulative Energy Demand (CED) in MJ_{eq},
- Global Warming Potential (GWP) in $kg\ CO_{2\_eq}$,
- Abiotic Depletion Potential of mineral, fossil and renewable resources (ADP) in $kg\ Sb_{eq}$,
- Particulate Matter (PM) in $kg\ PM2.5_{eq}$.

Each indicator represents one impact category that assesses effects on resource depletion, climate change, ecosystem quality and human health.

To compare the relative importance of each indicator, it is necessary to normalise them according to the coefficients given in Table 2. This normalisation gives the environmental impacts of the system in equivalent European habitants per year [38].

3. Optimisation of the thermocline storage system

3.1. Overall structure of the multi-criteria optimisation

Fig. 5 shows the link between the physical and the environmental models, described in the previous sections, based on different inputs and outputs of each model.

3.2. Optimisation algorithm

The optimisation problem is to find the optimal values of both shape factors according to given design parameters (Table 3). The parameters are set from the specifications of the thermocline tank to be optimised given in Table 1, i.e. the existing industrial thermocline tank (Fig. 2).

To solve this problem PSO algorithm [40,41], available in Matlab®, was chosen and the default parameters are kept.

The objective function, called the fitness function, includes the two criteria with their respective weighting factors (Eq. (15)). The algorithm tries to minimise this function to find the best geometry of the TES system according to the chosen HTF and TESM. LCA criterion includes the four indicators chosen for this study: GWP, CED, ADP of mineral, and PM. It is defined as the sum of these normalised indicators in order to have a single environmental optimisation criterion. In the following sections, this environmental criterion is given for the lifetime of the thermocline TES.

$$fitness = LCA{\cdot}\omega_{LCA} - \eta_{ex}{\cdot}\omega_{ex} \tag{15}$$

The weight of each criterion allows the relative importance of the two criteria to be varied. In this study, different weighting factors will be used to plot the Pareto fronts of the optimised solutions. The LCA weight is set to unity while the exergy weight ranges from 1 to 10 000 (Table 4).

To resume, the optimisation problem is given by:

$$Min(fitness)\ \ with\ \begin{cases} (Ex_{ds})^{*} = (Ex_{ds})_{ES} \\ \varepsilon = 40\%\ \ and\ \ \tau_{cutoff} = 20\% \\ T_H = 600^{\circ}C\ \ and\ \ T_L = 20^{\circ}C \end{cases} \tag{16}$$

Table 2
Normalised coefficients of indicators chosen - impacts of annual consumption and waste of an average European

Impact category	Indicator	Unit	Normalisation	Source
Energy	CED	MJ_{eq}	153 500	*Bilan Produit* – UE15 (2011) [39]
Climate change	*GWP*	$kg\ CO_{2\_eq}$	9 220	ILCD recommended normalisation factors for the EU-27 [38]
Resource depletion	ADP	$kg\ Sb_{eq}$	0.101	
Particulate matter	PM	$kg\ PM2.5_{eq}$	3.8	

4. Results and discussions

4.1. Application to the Eco-Stock® tank

The optimisation method is applied to an existing industrial thermocline tank depicted in Fig. 6. This is an air/ceramic packed-bed system with a maximum storage capacity of 10 GJ (2.8 MWh). Its specifications are reported in Table 5. The thermophysical properties of HTF and TESM are evaluated at average operating temperatures (310 °C). A lifetime of 25 years is assumed.

The physical model developed in [24] is applied on this industrial thermocline tank to simulate successive charge–discharge cycles. Fig. 7a presents the simulated temperature profiles at the end of the charging and discharging processes for six successive cycles.

Starting from a fully discharged state (cycle 1), the temperature profiles become less and less steep, cycle after cycle, implying a widening of the thermocline zone, and consequently, a decrease of the thermal energy flowing in and out of the system (Fig. 7b). A stationary periodic evolution is reached after six cycles, with a cycle time (charge/discharge) of 8.3 hours. The storage performances are evaluated on this last cycle.

LCA is also applied to the reference tank. Table 6 presents the exergy and LCA indicators obtained for the reference thermocline tank. LCA tot. is the sum of the four normalised indicators following the ILCD method [38].

4.2. Single-criterion optimisations

Fig. 8 shows the temperature profiles of the reference and the two optimised tanks as functions of their normalised lengths. The blue, green

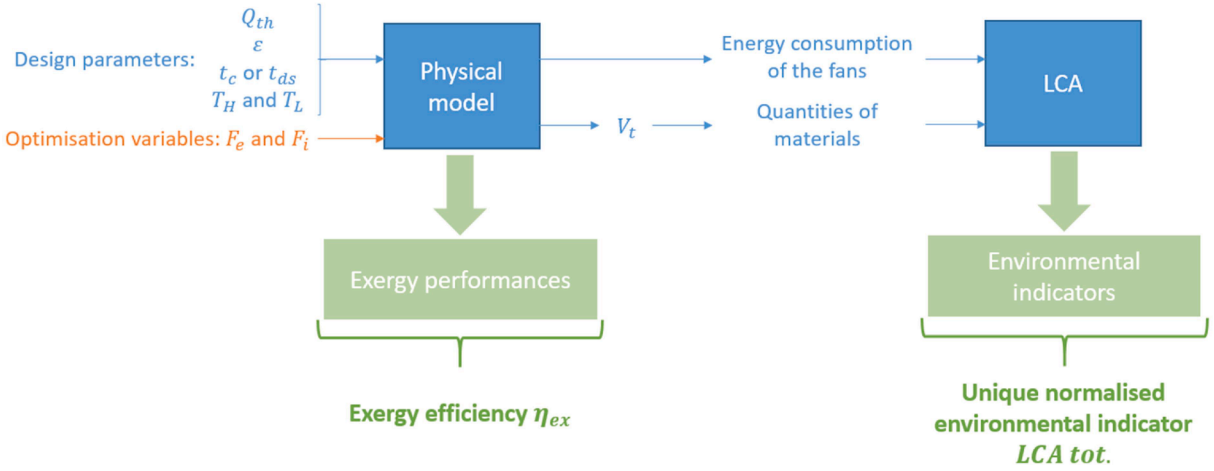

Fig. 5. Overall structure of the multi-criteria optimisation with the inputs and outputs of each model

Table 3
Optimisation problem definition

Constraints	Variables	Type	Range
Porosity	External shape factor	Continuous	[0.1; 3]
Operating temperatures	Internal shape factor	Continuous	[0.0001; 0.5]
Cut-off rate			

and red colours refer respectively to the reference tank, the exergy-optimised tank and the LCA-optimised tank. Same colour codes will be used in the following sections.

The two criteria lead to different optimised solutions. This is illustrated by the temperature profiles. The exergy optimisation leads to steeper temperature profiles than those obtained for the reference tank or the LCA-optimised tank. This results in a larger active storage zone, which is bounded by the two temperature profiles obtained at the end of the charging/discharging processes. Consequently, the utilisation ratio (Eq. (8)) is much better for the exergy-optimised tank (73.4%) than for the reference tank (56.8%). As the functional unit refers to the same amount of released exergy, better utilisation ratio will lead to smaller tank volume. Looking at the temperature profiles, the LCA optimisation appears to be a compromise between the exergy-optimised tank and the reference tank. A utilisation ratio of 67.5% is obtained. As a first conclusion, it can be stated that both optimisations result in the TES volume reduction, and that the exergy optimisation leads to greater decrease than the environmental optimisation. This better utilisation ratio also implies an increase in cycle durations passing from 8.3 h for the reference tank to 9.7 h for the LCA optimisation and 10.5 h for the exergy optimisation.

To clarify these trends, Fig. 9 presents the four LCA indicators for the reference tank, the exergy-optimised tank and the LCA-optimised tank. For each indicator, the impact of the different life cycle phases is indicated as well as the total normalised environmental impacts (LCA tot.). The transport and end-of-life phases are not very significant with less than 2% of the total environmental impacts. The tank construction accounts for almost 45% of the total impact while the filler material production and the use account for approximatively 29% for all three cases. Note that the use phase impact is much higher for the exergy-optimised tank than for the two other cases. It represents 31% of the total

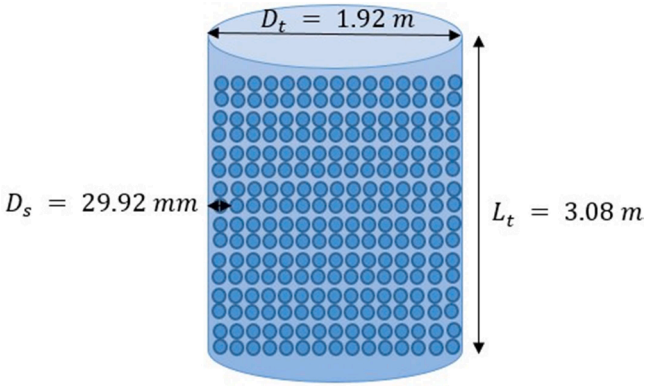

Fig. 6. Dimensions of the Eco-Stock® thermal storage system

Table 5
Specifications of the industrial thermocline tank

Parameters of the tank	Values
Maximum theoretical energy capacity Q_{th}	$10^{10}\ J$
Discharge exergy Ex_{ds}	707 $kWh/cycle$
Porosity ε	40%
Charge or discharge time t_c or t_{ds} (target values)	7.05 *hours*
Hot temperature T_H	$600^{\circ}C$
Low temperature T_L	$20^{\circ}C$
Ambient temperature T_∞	$15^{\circ}C$
HTF thermophysical properties (dry air)	$Cp_f = 1047.6\ J{\cdot}kg^{-1}{\cdot}K^{-1}$ $\rho_f = 0.595\ kg{\cdot}m^{-3}$ $\lambda_f = 0.045\ W{\cdot}m^{-1}{\cdot}K^{-1}$ $\mu_f = 2.1{\cdot}10^{-5}\ Pa{\cdot}s$
TESM thermophysical properties (ceramic)	$Cp_s = 1076\ J{\cdot}kg^{-1}{\cdot}K^{-1}$ $\rho_s = 3005\ kg{\cdot}m^{-3}$ $\lambda_s = 3.982\ W{\cdot}m^{-1}{\cdot}K^{-1}$
Cut-off rate τ_{cutoff}	20%
External shape factor F_e	0.6228
Internal shape factor F_i	0.0156

Table 4
Values of the exergy weight tested with PSO algorithm

Test	#1	#2	#3	#4	#5	#6	#7	#8	#9	#10
ω_{ex}	1	100	200	400	800	1 000	2 000	4 000	8 000	10 000

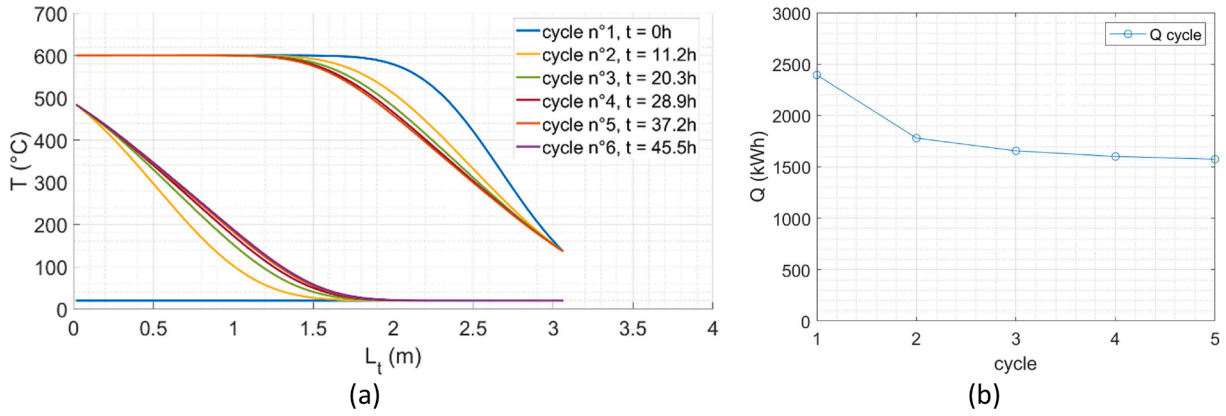

Fig. 7. Temperature limit profiles (a), Internal energy of the tank (b) for Eco-Stock® tank

Table 6
Results of the two models on the reference tank

Physical model		LCA	
η_{ex}	95.6%	$GWP\ (kg\ CO_{2\_eq})$	56 600
$\tau_{u,ex}$	56.8%	$CED\ (MJ_{eq})$	1 080 000
		$ADP\ (kg\ Sb_{eq})$	6.44
		$PM\ (kg\ PM2.5_{eq})$	52.7
		$LCA\ tot.\ (hab/year)$	91

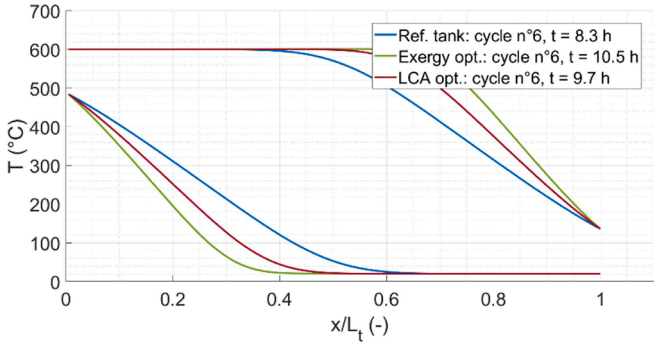

Fig. 8. Evolution of temperature limit profiles depending on the three studied tanks

normalised impacts compared to 16% and 21% respectively for the reference and LCA-optimised tanks. For TESM production, the opposite is observed with 24% of the total impacts for the exergy optimisation and 33% and 29% for the other configurations. The LCA optimisation reduces the normalised environmental impacts to 86 habitants per year, which is 13% less than the impact of the exergy-optimised tank.

The ADP indicator is the most impacting indicator with more than 66% of the total LCA impact. Indeed, the storage tank uses a lot of materials (steel, rock wool, aluminium, bauxite, etc.), components (piping, fans, pump, etc.) during the commissioning phase and energy to operate during its lifespan. The environmental impacts on the ADP indicator is detailed in Figs. 10 and 11. The mass of the tank and the filler materials is compared to the normalised impacts of the design phases. The normalised impacts of the tank and the TESM production are proportional to the masses of the various components. The mass of the tank is almost equal for all three cases. The mass of the solid particles is significantly lower in the case of the exergy optimisation, which results in less ADP during the solid particles production phase (Fig. 10). Indeed, the real volume of the exergy-optimised tank is reduced by 23% compared to the reference tank and by 16% for the LCA-optimised tank. However, the ADP induced by the use phase shows substantial differences between the three cases: this indicator is 1.6 times higher for the exergy-optimised tank than for the reference tank and the LCA-optimised tank. This is due to a larger pumping energy consumed by the exergy-optimised tank, which requires a lot of abiotic resources (Fig. 11). This fact is highlighted by analysing the GWP and CED indicators, which each account for slightly less than 10% of the total LCA

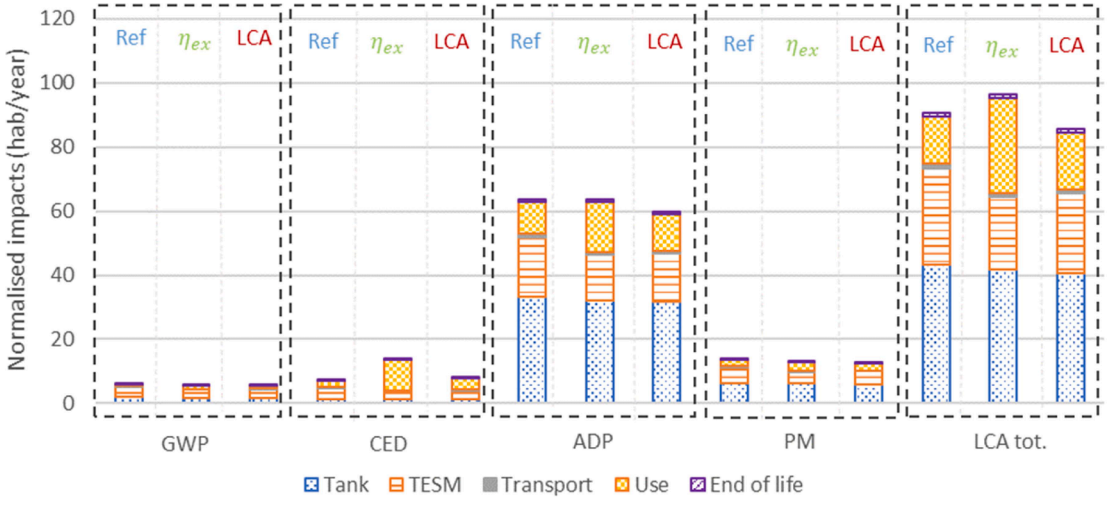

Fig. 9. Comparison of LCA normalised indicators for the different configurations by phases of the life cycle

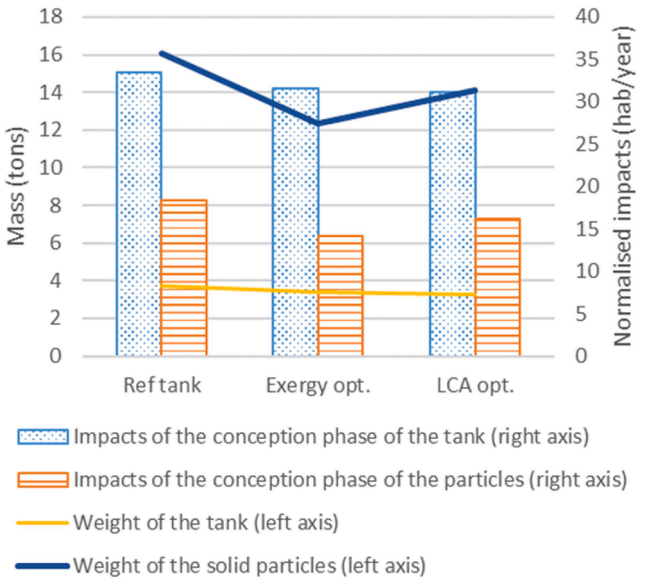

Fig. 10. Environmental impacts of the conception phases (tank and TESM) for the ADP indicator

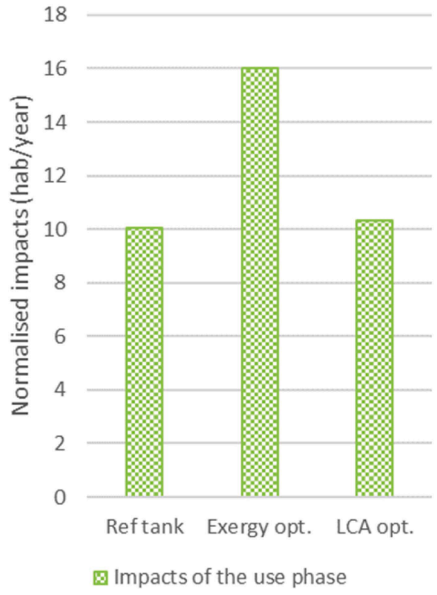

Fig. 11. Environmental impacts of the use phase for the ADP indicator

impact except for the exergy optimisation (Fig. 9). Both indicators are particularly influenced by the use phase of the TES (Fig. 9). In the exergy optimisation, the particle diameter is small (9.1 mm vs. 9.7 mm for the LCA optimisation) but the tank length is large (3.16 m vs. 2.23 m for the LCA optimisation), which leads to high pressure drop in the tank (almost 3 times higher than the LCA optimisation), and therefore a high pumping energy.

Fig. 12 shows the evolution of the mass and the real volume of the tank and the energy consumed by the fans. It shows that the mass and volume reduction related to the exergy optimisation is paid by a large increase in pumping energy. As a consequence, the exergy optimisation increases the CED indicator by 1.8 times compared to the LCA optimisation.

The results of the different optimisations are given in Table 7.

4.3. *Two-criteria optimisation*

This section focuses on the combined exergy/LCA optimisation. Fig. 13 shows the Pareto set obtained by varying the exergy weighting factors, and the reference tank indicators. This Pareto set is bounded by the exergy optimisation – on the right of the Pareto graph – and the LCA optimisation – on the left. The results of the reference tank do not belong to the Pareto set. This proves that it is possible to optimise the industrial tank to achieve better storage performances.

The different simulations indicate that the higher the exergy weight, the higher the exergy efficiency, with an exponential increase in environmental impacts. The influence of the exergy weight does not really begin until a value of 100. Looking at the Pareto set, the point [0.970; 87] seems interesting because the environmental impacts remain low for a good exergy efficiency. Indeed, this point is located before a strong degradation of the LCA criterion while being at 0.0017 points away from the exergy efficiency optimum. Thus, the exergy weight of 1000 seems to provide a good compromise for these two optimisation criteria. For this weighting factor, the diameter and the length of the thermocline tank are respectively 2.00 m and 2.31 m for a particle diameter of 8.6 mm. This geometry corresponds to an external shape factor of 0.865 as illustrated below. The different performance indicators and parameters of this tank, named exergy-LCA optimisation, are presented in Table 7

Fig. 14 shows the different shape factors of the 10 weighting factors, the optimised tanks and the reference tank. The internal shape factor evolves between 0.004 and 0.006 as the exergy weighting factor increases. Conversely, the external shape factor decreases from 0.93 to 0.53. As investigated in the single criterion optimisation, it is larger for the environmental optimisation and smaller for the exergy optimisation. Therefore, increasing the external shape factor leads to an increase in the tank length and a decrease in its diameter. To sum up, as the exergy weight increases, the tank and solid diameters decrease, while the tank height increases (Fig. 15). Thence, the tank changes from a square shape (LCA optimisation) to a tapered shape (exergy optimisation).

5. Conclusion

This work focused on thermocline TES optimisation, combining exergy analysis and LCA. The proposed method is applied to an existing industrial air/ceramic packed-bed TES taking as reference case. The functional unit of the LCA is defined from this reference tank: provide the same discharged exergy during its lifespan.

The exergy optimisation improves the exergy efficiency of the reference TES system by 1.7% but increases its environmental impact by 6%: the CED is twice as high and the other indicators are similar. The GWP, PM, CED and ADP indicators represent respectively 6%, 14%, 14% and 66% of the total environmental impacts of the exergy-optimised tank. With regard to the environmental optimisation, the exergy efficiency is slightly higher than that of the reference tank (96.9% vs 95.6%), and the environmental impact decreases by 5 habitants per year. The GWP, ADP and PM indicators are reduced by almost 9% while CED indicator increases by 12%. Both optimisations lead to decrease the particle diameter, that induces higher pumping power.

This study seeks to find the optimal geometry of the thermocline tank for a given fluid and a filler material. To solve the multi-criteria problem, a PSO algorithm was used. Different weighting factors were tested to find the Pareto set, bounded by the exergy and the LCA optimisation.

With regard to the shape factors, increasing the exergy weighting factor leads to a decrease in the external shape factor. As the internal shape factor remains constant (close to 0.005), this implies a reduction in particle diameter and an increase in tank height. Thence, the shape of the tank changes from a square shape (LCA optimisation) to a tapered shape (exergy optimisation). This also leads to a better utilisation ratio, and consequently to a decrease in the tank volume.

A good compromise for these two optimisation criteria has been selected, corresponding to an exergy weighting factor of 1000. In this

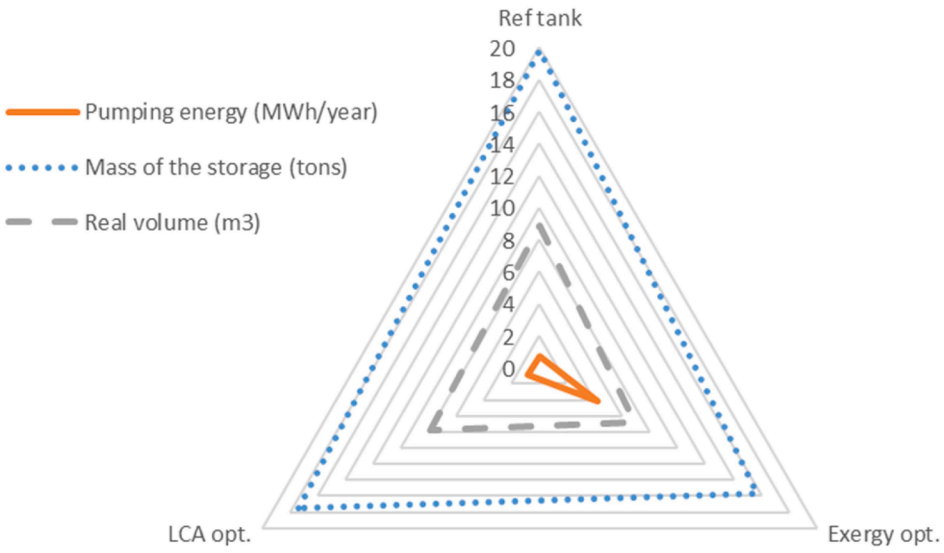

Fig. 12. Evolution of different parameters influencing LCA for the three studied tanks

Table 7
Summary of the dimensions, the exergy performances and the environmental impacts of the four different tanks

	Reference tank	Exergy optimisation	LCA optimisation	Exergy-LCA optimisation
F_e	0.6228	0.5250	0.9250	0.8652
F_i	0.0156	0.0055	0.0047	0.0043
D_t (m)	1.92	1.66	2.06	2.00
L_t (m)	3.08	3.16	2.23	2.31
D_s (mm)	29.9	9.1	9.7	8.6
V (m^3)	8.90	6.82	7.43	7.26
η_{ex}	95.6%	97.2%	96.9%	97.0%
$\tau_{u,ex}$	56.8%	73.5%	67.5%	69.1%
t_{cycle} (h)	8.3	10.5	9.7	9.9
GWP $(kg\ CO_{2\_eq})$	56 600	52 900	50 700	50 600
CED (MJ_{eq})	1 080 000	2 120 000	1 210 000	1 350 000
ADP $(kg\ Sb_{eq})$	6.44	6.45	6.04	6.07
PM $(kg\ PM2.5_{eq})$	53.7	49.7	47.7	47.7
$LCA\ tot.$ $(hab/year)$	91	97	86	87

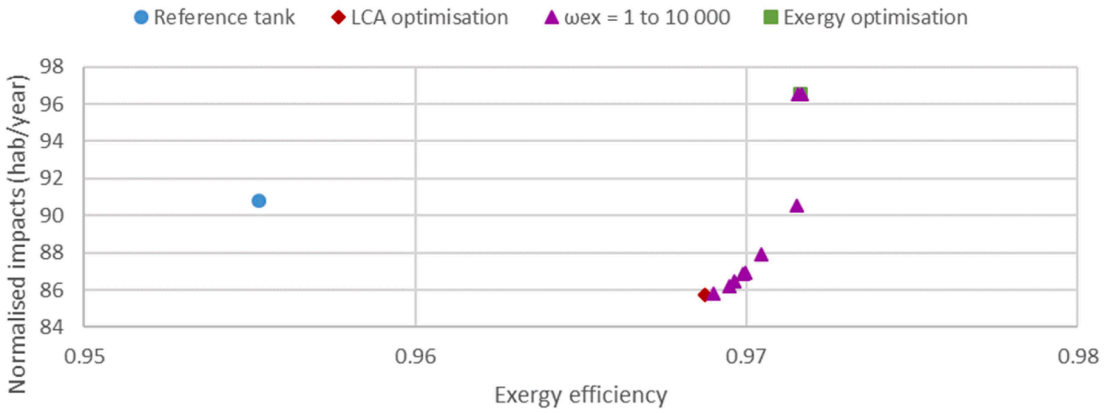

Fig. 13. Pareto graph of exergy/LCA optimisations with different weights

case, the normalised environmental impacts are 87 hab/year and the exergy efficiency is 97.0%. The proposed geometry is a thermocline tank with a diameter of 2.00 m, a length of 2.31 m and a particle diameter of 8.6 mm.

The next step will consist to select different HTF and solid filler materials and test them to find the best combination. In order to find the best and the most robust thermocline storage configuration on the Pareto set, multi-criteria decision support methods will be applied. TOPSIS [42], FUCA [43] and PROMETHEE [44] methods can be used. Thereafter, additional work will solve another multi-criteria

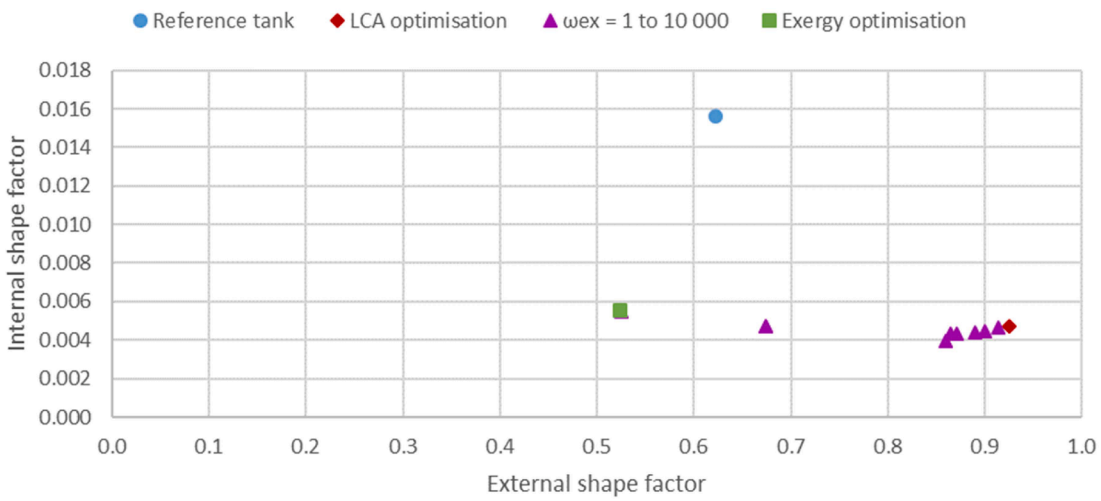

Fig. 14. Shape factors of exergy/LCA optimisations with different weights

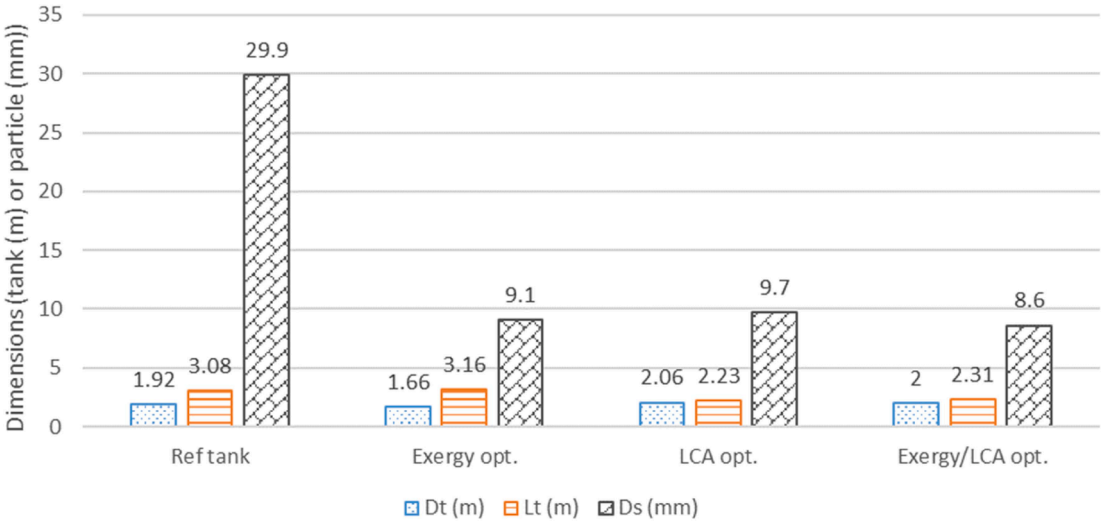

Fig. 15. Comparison between the three different designs: the reference (left), the exergy (middle) and the LCA (right) optimisations

optimisation problem, using levelized cost of energy as an optimisation criterion [45–48].

CRediT authorship contribution statement

D. Le Roux: Methodology, Software, Writing – original draft, Writing - review & editing, Investigation. **Y. Lalau:** Software, Methodology. **B. Rebouillat:** Software, Methodology, Validation. **P. Neveu:** Supervision, Resources, Writing - review & editing. **R. Olives:** Supervision, Resources, Writing - review & editing, Funding acquisition.

Declaration of Competing Interest

The authors declare that they have no known competing financial interests or personal relationships that could have appeared to influence the work reported in this paper.

Acknowledgements

This project has received funding from the Occitanie region under award number 19008845 ALDOCT 000791. The authors would like to thank Eco-Tech Ceram for sharing the data used in this study.

References

[1] REN21, Renewables 2019 Global Status Report. Paris: REN21 Secretariat, 2019. Accessed: Jun. 12, 2020. [Online]. Available: https://www.ren21.net/wp-content/uploads/2019/05/gsr_2019_full_report_en.pdf.

[2] Jouhara H, Olabi AG. Editorial: Industrial waste heat recovery. Energy 2018;160:1–2. https://doi.org/10.1016/j.energy.2018.07.013.

[3] ADEME, Excess heat, 2017th ed. Angers: ADEME, 2018. Accessed: Jun. 11, 2020. [Online]. Available: https://www.ademe.fr/excess-heat.

[4] Panayiotou GP, Bianchi G, Georgiou G, Aresti L, Argyrou M, Agathokleous R, et al. Preliminary assessment of waste heat potential in major European industries. Energy Procedia 2017;123:335–45. https://doi.org/10.1016/j.egypro.2017.07.263.

[5] Eurostat, Energy balance sheets - 2017 data. Luwembourg: Publications Office of the European Union, 2019. Accessed: Dec. 08, 2020. [Online]. Available: https://ec.europa.eu/eurostat/documents/3217494/10077623/KS-EN-19-001-EN-N.pdf/59b44e6f-ff33-488b-a85f-9c4f60703afc.

[6] Papapetrou M, Kosmadakis G, Cipollina A, La Commare U, Micale G. Industrial waste heat: Estimation of the technically available resource in the EU per industrial sector, temperature level and country. Appl Therm Eng 2018;138:207–16. https://doi.org/10.1016/j.applthermaleng.2018.04.043.

[7] Su Z, Zhang M, Xu P, Zhao Z, Wang Z, Huang H, et al. Opportunities and strategies for multigrade waste heat utilization in various industries: A recent review. Energy Convers Manag 2021;229:113769. https://doi.org/10.1016/j.enconman.2020.113769.

[8] Miró L, Gasia J, Cabeza LF. Thermal energy storage (TES) for industrial waste heat (IWH) recovery: A review. Appl Energy 2016;179:284–301. https://doi.org/10.1016/j.apenergy.2016.06.147.

[9] López-Sabirón AM, Aranda-Usón A, Mainar-Toledo MD, Ferreira VJ, Ferreira G. Environmental profile of latent energy storage materials applied to industrial systems. Sci Total Environ 2014;473–474:565–75. https://doi.org/10.1016/j.scitotenv.2013.12.013.

[10] Rahman MM, Oni AO, Gemechu E, Kumar A. Assessment of energy storage technologies: A review. Energy Convers Manag 2020;223:113295. https://doi.org/10.1016/j.enconman.2020.113295.

[11] Fasquelle T, Falcoz Q, Neveu P, Hoffmann J-F. Numerical simulation of a 50 MWe parabolic trough power plant integrating a thermocline storage tank. Energy Convers Manag 2018;172:9–20. https://doi.org/10.1016/j.enconman.2018.07.006.

[12] Heath G, Turchi C, Decker T, Burkhardt J, Kutscher C, "Life Cycle Assessment of Thermal Energy Storage: Two-Tank Indirect and Thermocline," in ASME 2009 3rd International Conference on Energy Sustainability, Volume 2, San Francisco, California, USA, 2009, pp. 689–690. doi: 10.1115/ES2009-90402.

[13] Galione P, Pérez-Segarra C, Rodríguez I, Torras S, Rigola J. Numerical evaluation of multi-layered solid-PCM thermocline-like tanks as thermal energy storage systems for CSP applications. Energy Procedia 2015;69:832–41. https://doi.org/10.1016/j.egypro.2015.03.099.

[14] Pacheco JE, Showalter SK, Kolb WJ. Development of a molten-salt thermocline thermal storage system for parabolic trough plants. J Sol Energy Eng 2002;124(2):153–9. https://doi.org/10.1115/1.1464123.

[15] Brosseau D, Kelton JW, Ray D, Edgar M, Chisman K, Emms B. Testing of thermocline filler materials and molten-salt heat transfer fluids for thermal energy storage systems in parabolic trough power plants. J Sol Energy Eng 2005;127(1):109–16. https://doi.org/10.1115/1.1824107.

[16] Lavan Z, Thompson J. Experimental study of thermally stratified hot water storage tanks. Sol Energy 1977;19(5):519–24. https://doi.org/10.1016/0038-092X(77)90108-6.

[17] Faas SE, Thorne LR, Fuchs EA, Gilbertsen ND. "MWe Solar Thermal Central Receiver Pilot Plant: Thermal Storage Subsystem Evaluation," in: Report No. SAND86-8212, Sandia National Laboratories Livermore, CA, 1986.

[18] Hoffmann J-F, Fasquelle T, Goetz V, Py X. A thermocline thermal energy storage system with filler materials for concentrated solar power plants: Experimental data and numerical model sensitivity to different experimental tank scales. Appl Therm Eng 2016;100:753–61. https://doi.org/10.1016/j.applthermaleng.2016.01.110.

[19] Ammar ASA, Ghoneim AA. Optimization of a sensible heat storage unit packed with spheres of a local material. Renew Energy 1991;1(1):91–5. https://doi.org/10.1016/0960-1481(91)90107-Z.

[20] Bejan A. Entropy generation through heat and fluid flow. J Appl Mech 1982;50:475.

[21] Krane RJ. A Second Law analysis of the optimum design and operation of thermal energy storage systems. Int J Heat Mass Transf 1987;30(1):43–57. https://doi.org/10.1016/0017-9310(87)90059-7.

[22] Biyikoğlu A. Optimization of a sensible heat cascade energy storage by lumped model. Energy Convers. Manag. 2002;43(5):617–37. https://doi.org/10.1016/S0196-8904(01)00061-9.

[23] Flueckiger SM, Garimella SV. Second-law analysis of molten-salt thermal energy storage in thermoclines. Sol Energy 2012;86(5):1621–31. https://doi.org/10.1016/j.solener.2012.02.028.

[24] Rebouillat B, Falcoz Q, Neveu P. "2nd law analysis of thermocline – heat storage system," in ECOS 2019, Wrocław, Poland, Jun. 2019, pp. 3065–3076. [Online]., ISBN: 978-83-61506-51-5, Available: http://www.s-conferences.eu/ecos2019.

[25] Haller MY, Cruickshank CA, Streicher W, Harrison SJ, Andersen E, Furbo S. Methods to determine stratification efficiency of thermal energy storage processes – Review and theoretical comparison. Sol Energy 2009;83(10):1847–60. https://doi.org/10.1016/j.solener.2009.06.019.

[26] Rosen MA. The exergy of stratified thermal energy storages. Sol Energy 2001;71(3):173–85. https://doi.org/10.1016/S0038-092X(01)00036-6.

[27] International Organization for Standardization, "ISO 14040 - Environmental management — Life cycle assessment — Principles and framework," British Standard Institution, BS EN ISO 14040:2006+A1:2020, Nov. 2020. Accessed: May 20, 2020. [Online]. Available: https://landingpage.bsigroup.com/LandingPage/Undated?UPI=000000000001139131.

[28] Oró E, Gil A, de Gracia A, Boer D, Cabeza LF. Comparative life cycle assessment of thermal energy storage systems for solar power plants. Renew Energy 2012;44:166–73. https://doi.org/10.1016/j.renene.2012.01.008.

[29] Lalau Y, Py X, Meffre A, Olives R. Comparative LCA between current and alternative waste-based TES for CSP. Waste Biomass Valorization 2016;7(6):1509–19. https://doi.org/10.1007/s12649-016-9549-6.

[30] Nahhas T, Py X, Olives R. Life cycle assessment of air-rock packed bed storage system and its comparison with other available storage technologies for concentrating solar power plants. Waste Biomass Valorization 2018;11(5):2357–65. https://doi.org/10.1007/s12649-018-0529-x.

[31] Garg P, Orosz MS. Economic optimization of Organic Rankine cycle with pure fluids and mixtures for waste heat and solar applications using particle swarm optimization method. Energy Convers Manag 2018;165:649–68. https://doi.org/10.1016/j.enconman.2018.03.086.

[32] Touzo A, Olives R, Dejean G, Pham Minh D, El Hafi M, Hoffmann J-F, et al. Experimental and numerical analysis of a packed-bed thermal energy storage system designed to recover high temperature waste heat: an industrial scale up. J. Energy Storage 2020;32:101894. https://doi.org/10.1016/j.est.2020.101894.

[33] Eco-Tech Ceram, "ecotechceram.com," Eco-Tech Ceram. https://www.ecotechceram.com/ (accessed Oct. 26, 2020).

[34] Wakao N, Kaguei S, Funazkri T. Effect of fluid dispersion coefficients on particle-to-fluid heat transfer coefficients in packed beds: Correlation of nusselt numbers. Chem Eng Sci 1979;34(3):325–36. https://doi.org/10.1016/0009-2509(79)85064-2.

[35] Ecoinvent, "ecoinvent.org," Ecoinvent. https://www.ecoinvent.org/ (accessed Jul. 29, 2021).

[36] "openLCA.org," OpenLCA. https://www.openlca.org/ (accessed Jul. 29, 2021).

[37] Lalau Y. , Al Alsmi I. , Olivès R. , Dejean G. , Meffre A. , Py X. (in press). May an energy efficiency system be environmentally detrimental? An LCA and net energy approach . Journal of Cleaner Production.

[38] European Commission, Joint Research Centre, and Institute for Environment and Sustainability, International reference life cycle data system (ILCD) handbook general guide for life cycle assessment: provisions and action steps., First Edition. Luxembourg: Publications Office of the European Union, 2011. [Online]. Available: https://eplca.jrc.ec.europa.eu/uploads/ILCD-Recommendation-of-methods-for-LCIA-def.pdf.

[39] ADEME, "base-impacts.ademe," Base-Impacts(R). http://www.base-impacts.ademe.fr/bilan-produit (accessed Jul. 29, 2021).

[40] Kennedy J, Eberhart R, "Particle swarm optimization," in Proceedings of ICNN'95 - International Conference on Neural Networks, Perth, WA, Australia, Nov. 1995, vol. 4, pp. 1942–1948. doi: 10.1109/ICNN.1995.488968.

[41] Wang D, Tan D, Liu L. Particle swarm optimization algorithm: an overview. Soft Comput 2018;22(2):387–408. https://doi.org/10.1007/s00500-016-2474-6.

[42] Brans JP, Vincke P, Mareschal B. How to select and how to rank projects: The Promethee method. Eur J Oper Res 1986;24(2):228–38. https://doi.org/10.1016/0377-2217(86)90044-5.

[43] Mendoza M, F.L., Perez Escobedo JL, Azzaro-Pantel C, Pibouleau L, Domenech S, Aguilar-Lasserre A. "Selecting the best portfolio alternative from a hybrid multiobjective GA-MCDM approach for New Product Development in the pharmaceutical industry," in: 2011 IEEE Symposium on Computational Intelligence in Multicriteria Decision-Making (MDCM), Apr. 2011, pp. 159–166. doi: 10.1109/SMDCM.2011.5949271.

[44] Hwang C-L, Yoon K. Multiple attribute decision making: methods and applications : a state-of-the-art survey. Berlin, New York: Springer-Verlag; 1981.

[45] Aussel D, Neveu P, Tsuanyo D, Azoumah Y. On the equivalence and comparison of economic criteria for energy projects: Application on PV/diesel hybrid system optimal design. Energy Convers Manag 2018;163:493–506. https://doi.org/10.1016/j.enconman.2017.12.050.

[46] Azoumah YK, Tossa AK, Dake RA. Towards a labelling for green energy production units: Case study of off-grid solar PV systems. Energy 2020;208:118149. https://doi.org/10.1016/j.energy.2020.118149.

[47] Ahmed N, Elfeky KE, Lu L, Wang QW. Thermal and economic evaluation of thermocline combined sensible-latent heat thermal energy storage system for medium temperature applications. Energy Convers Manag 2019;189:14–23. https://doi.org/10.1016/j.enconman.2019.03.040.

[48] Xie N, Liu Z, Luo Z, Ren J, Deng C, Yang S. Multi-objective optimization and life cycle assessment of an integrated system combining LiBr/H2O absorption chiller and Kalina cycle. Energy Convers Manag 2020;225:113448. https://doi.org/10.1016/j.enconman.2020.113448.